JOURNAL OF VIROLOGY, Nov. 2011, p. 11601–11614 Vol. 85, No. 22
0022-538X/11/$12.00 doi:10.1128/JVI.05239-11

HIV-1 Coinfection and Morphine Coexposure Severely Dysregulate Hepatitis C Virus-Induced Hepatic Proinflammatory Cytokine Release and Free Radical Production: Increased Pathogenesis Coincides with Uncoordinated Host Defenses▽

Nazira El-Hage,[1]* Seth M. Dever,[1] Sylvia Fitting,[1] Tasrif Ahmed,[1] and Kurt F. Hauser[1,2]

Department of Pharmacology and Toxicology, Virginia Commonwealth University, Medical College of Virginia Campus, Richmond, Virginia 23298,[1] and Institute for Drug and Alcohol Studies, Virginia Commonwealth University, Richmond, Virginia 23298[2]

Received 27 May 2011/Accepted 28 August 2011

Coinfection with human immunodeficiency virus type-1 (HIV-1) and hepatitis C virus (HCV) is a global problem that is more prevalent in injection drug users because they have a higher risk for acquiring both viruses. The roles of inflammatory cytokines and oxidative stress were examined in HIV-1- and HCV-coinfected human hepatic cells. Morphine (the bioactive product of heroin), HIV-1 Tat and the MN strain gp120 ($gp120_{MN}$) proteins, and X4 HIV-$1_{LAI/IIIB}$ and R5 HIV-1_{SF162} isolates were used to study the mechanisms of disease progression in HCV (JFH1)-infected Huh7.5.1 cell populations. HCV increased tumor necrosis factor-α (TNF-α) and interleukin-6 (IL-6) release and augmented production of reactive oxygen species (ROS), nitric oxide (NO), and 3-nitrotyrosine (3-NT) in Huh7.5.1 cells. Morphine preferentially affected R5-tropic, but not X4-tropic, HIV-1 interactions with Huh7.5.1 cells. HIV-1 proteins or isolates increased cytokine release in HCV-infected cells, while adding morphine to coinfected cells caused complex imbalances, significantly disrupting cytokine secretion depending on the cytokine, morphine concentration, exposure duration, and particular pathogen involved. Production of ROS, NO, and 3-NT increased significantly in HCV- and HIV-1-coexposed cells while exposure to morphine further increased ROS. The proteasome inhibitor MG132 significantly decreased oxyradicals, cytokine levels, and HCV protein levels. Our findings indicate that hepatic inflammation is increased by combined exposure to HCV and HIV-1, that the ubiquitin-proteasome system and NF-κB contribute to key aspects of the response, and that morphine further exacerbates the disruption of host defenses. The results suggest that opioid abuse and HIV-1 coinfection each further accelerate HCV-mediated liver disease by dysregulating immune defenses.

Among injection drug users (IDUs), human immunodeficiency virus type-1 (HIV-1) and hepatitis C virus (HCV) are the most frequently transmitted blood-borne pathogens. Approximately 180 million people are infected with HCV worldwide; of these, 1 million die each year of liver disease and/or liver cancer. In the United States alone, an estimated 2% of persons with chronic HCV infection (8,000 to 10,000) die of liver cancer annually (1, 61). HCV infection is characterized by a systemic increase in oxidative stress that is most likely caused by a combination of chronic inflammation, iron overload, liver damage, and proteins encoded by HCV (10, 58). Yet, despite the severity of its actions, HCV is typically noncytopathic (7, 8, 18, 63). Thus, the ensuing local necroinflammatory response, fibrogenesis, and possible cirrhosis are thought to result from generalized inflammation that may be influenced by comorbid diseases or xenobiotics (7, 8, 18, 63). In the United States, approximately 150,000 to 300,000 people are coinfected with HIV-1 and HCV. This represents 15 to 30% of all HIV-1-infected patients and 5 to 10% of all HCV patients (56, 60). HIV-1- and HCV-coinfected individuals have higher morbidity and mortality rates due to liver disease (68). In fact, coinfection with HIV-1 leads to accelerated hepatic fibrosis progression, with higher rates of cirrhosis, liver failure, and liver death, than mono-infection with HCV (5, 28, 53, 64).

Although little is known about the mechanisms by which HIV-1 and HCV directly interact at cellular and molecular levels, recent studies using direct virus-virus interactions *in vitro* provide additional insight into the events underlying the accelerated liver disease progression observed with HCV/HIV-1 coinfection (23, 32, 33, 68). Morphine, the major metabolite of heroin, is a prototypic opiate with abuse liability and is used clinically for pain management (13). Through the preferential activation of μ-opioid receptors, morphine influences a variety of physiological functions, including both innate and acquired immune responses (45, 48), which can result in increased susceptibility for bacterial and viral infections (67). More importantly, activation of the μ-opioid receptor can trigger increased production of reactive oxygen species (ROS) and induction of apoptosis (21), and morphine-induced oxidative damage has been hypothesized to contribute to many of the systemic manifestations of liver disease and hepatotoxicity seen experimentally in mice (43, 72), as well as in heroin abusers (59).

* Corresponding author. Mailing address: Department of Pharmacology and Toxicology, Virginia Commonwealth University School of Medicine, 1217 East Marshall Street, Richmond, VA 23298-0613. Phone: (804) 628-7573. Fax: (804) 827-9974. E-mail: nelhage@vcu.edu.

▽ Published ahead of print on 7 September 2011.

TABLE 1. List of antibodies used and their application to the present study

Antibody (primary reactivity and/or type)	Description (host)	Concn or dilution	Application[a]	Source (catalog no.)[b]
CD4 (human)	Polyclonal (rabbit)	1–2 μg/ml	WB	Abcam (ab-27452)
CXCR4 (human)	Polyclonal (rabbit)	0.5–2 μg/ml	WB	Abcam (ab-2074)
CKR-5 (D-6 or CCR5) (human)	Monoclonal (mouse)	1:500	WB	Santa Cruz (sc-17833)
β-Actin (human)	Monoclonal (mouse)	1:500	WB	Santa Cruz (sc-130300)
NF-κB p65 (human)	Monoclonal (mouse)	1:500	WB	Santa Cruz (sc-8008)
P~NF-κB p65 (human)	Polyclonal (rabbit)	1:500	WB	Santa Cruz (sc-101749)
NF-κB p50 (human)	Monoclonal (mouse)	1:500	WB	Santa Cruz (sc-53744)
P~NF-κB p50 (human)	Polyclonal (rabbit)	1:500	WB	Santa Cruz (sc-101745)
HCV NS3 (human)	Monoclonal (mouse)	1:1,000	WB	Abcam (ab-13830)
Fusin (4G10 or CXCR4) (human)	Monoclonal (mouse)	1:100	IF	Santa Cruz (sc-53534)
CCR5 (human)	Polyclonal (goat)	1:300	IF	Abcam (ab-1673)
HIV-1 p24 (human)	Monoclonal (mouse)	1:100	IF	Dako (M0857)
HCV core (human)	Monoclonal (mouse)	1:500	IF	Abcam (ab2740)
CD184 (CXCR4) (human)	APC-conjugated monoclonal (mouse)[c]	5 μg/ml	FC	BioLegend (306510)
CD195 (CCR5) (human)	Alexa Fluor 488-conjugated monoclonal (rat)[c]	5 μg/ml	FC	BioLegend (313710)
Isotype control (mouse)	Alexa Fluor 488-conjugated monoclonal (mouse)[c]	5 μg/ml	FC	BioLegend (400233)

[a] WB, Western blotting; IF, immunofluorescence; FC, flow cytometry.
[b] Supplier locations are as follows: Abcam, San Francisco, CA; Santa Cruz, Santa Cruz, CA; Dako, Carpinteria, CA; BioLegend, San Diego, CA.
[c] Detected by direct immunofluorescence with chromophores conjugated to the primary antibodies. All other antigens were detected by indirect immunofluorescence using appropriate secondary antibodies. APC, allophycocyanin.

Because of possible interactions between multiple harmful agents, including HIV-1, HCV, and morphine, we postulated that HIV-1-induced pathogenesis of HCV is aggravated by opioids. Our hypothesis was tested using an infectious HCV JFH1 cell culture model (65, 75). The results show the following: (i) that HCV JFH1 and HIV-1 trigger the release of proinflammatory molecules, tumor necrosis factor-α (TNF-α), interleukin-6 (IL-6), and RANTES (regulated on activation normal T-cell expressed and secreted) and increase the production of nitric oxide (NO), ROS, and 3-nitrotyrosine (3-NT); (ii) that exposure to morphine increases HIV-1 viral entry in Huh7.5.1 cells, exacerbates virally induced TNF-α and RANTES release, and increases the production of ROS and NO in HCV JFH1-infected hepatocytes; and (iii) that inhibition of the cellular proteasome attenuates HCV protein levels and diminishes the release of proinflammatory cytokines from HCV-infected Huh7.5.1 cells.

MATERIALS AND METHODS

Cell culture and HCV virus production. Huh (human hepatocellular carcinoma) cell line (Huh-7) and Huh-8 cells, which contain the HCV subgenomic replicon expressing nonstructural (NS) proteins (NS2, NS3, NS4A, NS4B, NS5A, and NS5B), were kindly provided by Wen-Zhe Ho (Temple University, Philadelphia, PA). Francis V. Chisari (The Scripps Research Institute, La Jolla, CA) kindly provided Huh7.5.1 cells. Cells were cultured in Dulbecco's modified Eagle's medium supplemented with 10% heat-inactivated fetal bovine serum, 100 nM nonessential amino acids, 100 U/ml penicillin, and 100 μg/ml streptomycin at 37°C in 5% CO_2–95% air. Cells containing the subgenomic HCV RNA were maintained in the presence of 300 μg/ml G418 (30) (Geneticin; Invitrogen, Carlsbad, CA) and passaged once per week. Peripheral blood mononuclear cells (PBMCs) were purchased from Astarte Biologics (Redmond, WA) and maintained in RPMI medium supplemented with 10% heat-inactivated fetal bovine serum, 100 U/ml penicillin, and 100 μg/ml streptomycin and incubated as indicated above. JFH1 HCV (genotype 2a infectious HCV isolate) and a replication-deficient mutant clone (JFH1/GND) were kindly provided by Takaji Wakita (National Institute for Infectious Diseases, Tokyo, Japan) and were prepared and used to infect Huh7.5.1 cells as previously reported (65, 75). At 72 h posttransfection, naïve Huh7.5.1 cells were inoculated with JFH1- and JFH1/GND-containing culture supernatants, and reverse transcription-PCR (RT-PCR) and immunofluorescence labeling were used to confirm that the newly inoculated cells were infected with JFH1 virus. The HCV JFH1 cells used in this study were harvested between days 5 to 7 postinfection, and the supernatants were stored at −70°C after filtration. Virus stocks were assayed for HCV core protein using a QuickTiter HCV core antigen enzyme-linked immunosorbent assay (ELISA) kit from Cell Biolabs (San Diego, CA).

Cell treatments. Mock- and JFH1-infected Huh7.5.1 cells (multiplicity of infection [MOI] of 1.0) were seeded overnight (14 h). Cells were treated the next day with morphine (50 nM, 500 nM, or 5,000 nM), Tat (10 nM, 100 nM, or 1,000 nM), or gp120 (50 pM, 500 pM, or 5,000 pM) alone or with increasing concentrations (50, 500, or 5,000 pg/ml HIV-1 p24 per 10^6 cells) of X4-tropic HIV-$1_{LAI/IIIB}$ or R5-tropic HIV-1_{SF162} isolates with or without morphine for 8 h, 24 h, and 72 h. X4-tropic HIV-$1_{LAI/IIIB}$ and X4-tropic HIV-1_{NL4-3} proviral plasmid DNAs were kind gifts from Fatah Kashanchi (George Mason University, Manassas, VA). R5-tropic HIV-1_{SF162} originally isolated by Jay Levy (9) and enhanced green fluorescent protein (EGFP)-Vpr plasmid (catalog number 11386) were obtained through the NIH AIDS Research and Reference Reagent Program (Germantown, MD). HIV-1_{NL4-3} proviral DNA and EGFP-Vpr plasmids were cotransfected at equal molar ratios into HEK-293T cells using Lipofectamine 2000 (Invitrogen) to create HIV-1_{NL4-3}-Vpr-GFP-labeled virions as previously described (51). R5-tropic BaL virions were also created by transfecting HEK-293T cells with pWT/BaL (catalog number 11414; NIH AIDS Research and Reference Reagent Program). The pBlue3′LTR-luc (where LTR is long terminal repeat) plasmid was obtained from the NIH AIDS Research and Reference Reagent Program (catalog number 4788). The HIV-1 coreceptor antagonists AMD3100 (100 nM) (CXCR4; Sigma-Aldrich, St. Louis, MO) and maraviroc (100 nM) (CCR5; a kind gift from Yan Zhang; Virginia Commonwealth University) were added 30 to 60 min prior to HIV-1 infection to selectively block viral entry. HIV-1 and morphine were added to cells at the same time. Mock-treated cells served as controls and provided background values against which JFH1-infected cell values were normalized. The working concentration of morphine was 500 nM. HIV-1 Tat and gp120 were used at 100 nM and 500 pM concentrations, respectively. The concentrations used were based on prior assessment of concentration-dependent effects in Huh-7 and Huh-8 cells.

Reagents. HIV-1 Tat recombinant protein consisting of residues 1 to 72 ($Tat_{1–72}$) was obtained from Philip Ray (University of Kentucky) and Avindra Nath (Johns Hopkins University), and dual-tropic gp120 protein from HIV-1 strain MN ($gp120_{MN}$) was purchased from ProSpec (East Brunswick, NJ). Morphine sulfate was obtained from the National Institute on Drug Abuse (NIDA; Drug Supply System, Bethesda, MD). The antibodies used, their titers or concentrations, applications, and sources are listed in Table 1. To explore the possible pathways of virus-induced production of ROS and cytokine release, mock- and JFH1-infected cells were preincubated with pathway inhibitors, including 10 μM *N*-acetyl cysteine (NAC, a precursor of glutathione; the thiol group of NAC can reduce free radicals) and 10 μM carbobenzoxy-L-leucyl-L-leucyl-L-leucinal

(MG132 or Z-LLL-CHO, a potent inhibitor of proteasome activity) for 30 to 60 min at 37°C prior to exposure to HIV-1 and opioids. Both inhibitors were purchased from EMD Chemicals (Rockland, MA). Unless stated, we followed the manufacturer's protocol when using manufactured kits.

Viral replication. Phytohemagglutinin (PHA)-activated PBMCs were infected with HIV-$1_{LAI/IIIB}$ and HIV-1_{SF162} at concentrations of 53 ng/ml and 74 ng/ml, respectively. The cell culture supernatants/conditioned media were harvested, filtered, and stored at −80°C. Viral stocks were quantified by assaying for HIV-1 p24 (Alliance p24 Antigen ELISA Kit; Advanced Bioscience, Kensington, MD).

Immunofluorescence microscopy. To monitor infection in the JFH1-exposed cell population, mouse anti-HCV core primary antibody (Table 1) and secondary goat anti-mouse antibodies conjugated to Alexa Fluor 488 (Invitrogen) were used to detect HCV core protein by standard immunofluorescence. Cells were counterstained with 4′,6′-diamidino-2-phenylindole (DAPI) to visualize nuclei, and fluorescently labeled cells were visualized using a Zeiss Axio Observer Z.1 microscope, Axio Vision (version 4.6) software, and an MRm digital camera (Carl Zeiss, Inc., Thornwood, NY).

Flow cytometry. CXCR4 and CCR5 immunoreactivity were detected by direct immunofluorescence in Huh7.5.1 cells by using flow cytometry. Huh7.5.1 cells were washed in phosphate-buffered saline (PBS)–0.1% bovine serum albumin (BSA) buffer and incubated with allophycocyanin (APC)-conjugated anti-CXCR4 and Alexa Fluor 488-tagged anti-CCR5 antibodies in permeabilization buffer (PBS–0.1% BSA–0.1% Triton X) to detect surface and intracellular expression. Fluorescence was measured from 10,000 gated Huh7.5.1 cells per treatment in each experiment using a FACSCanto II flow cytometer (BD Biosciences, San Jose, CA). Autofluorescence was compensated by setting the detector voltage to the minimum level that discriminates between autofluorescence and specific immunofluorescence in both negative and positive controls. Isotype control antibodies were used to define settings in histogram plot analyses (Table 1).

HIV-1 infection of Huh7.5.1 cells. Four different methods were used to monitor HIV-1 infectivity in Huh7.5.1 hepatic cells. Mouse anti-p24 primary antibody (Table 1) and secondary goat anti-mouse antibodies conjugated to Texas Red (Invitrogen) were initially used to detect HIV-1 p24 by standard immunofluorescence. Cells were counterstained with DAPI to visualize nuclei, and fluorescently labeled cells were visualized under fluorescence microscopy. In addition, Huh7.5.1 cells were infected with X4-tropic HIV-1_{NL4-3} carrying a Vpr-green fluorescent protein (HIV-1_{NL4-3} Vpr-GFP) or left uninfected for 3 h at 37°C, washed in PBS, fixed with 4% paraformaldehyde, and counterstained with DAPI. HIV-1_{NL4-3} Vpr-GFP-infected cells were imaged using a Zeiss LSM 700 laser scanning confocal microscope equipped with a 63× (1.42 numerical aperture [NA]) objective, using 488-nm laser excitation with dichroic beam-splitter set at 492 nm to optimize green fluorescent protein detection. The confocal images shown are optical sections from a single Z plane with the acquisition parameters, including the scan step (0.286 μm) and pinhole size (34 μm), set to optimize X-, Y-, and especially Z-plane resolution (Zen 2010 software; Zeiss). A third approach to monitor HIV-1 infectivity was to transfect Huh7.5.1 cells with a Tat-responsive HIV-1 long terminal repeat (LTR)-luciferase reporter plasmid (pBlue3′LTR-luc) using Lipofectamine 2000 (Invitrogen). After a 12-h inoculation with HIV-$1_{LAI/IIIB}$ or HIV-1_{SF162}, a rinse with fresh medium, and 48 h of incubation, HIV-1 Tat protein expression was assessed by luciferase activity using a Luciferase Assay System (Promega). A fourth strategy was to extract RNA from HIV-1-exposed Huh7.5.1 cells and subsequently measure Tat RNA expression by RT-PCR using the primers 5′-GCG GAT CCA TGG AGC CAG TAG ATC CTA G-3′ and 5′-T TAT CAT TGC TTT GAT AGA GAA ACT TG-3′.

Cytokine release. The effects of subgenomic HCV RNA on cytokine release by Huh-8 cells were initially screened using a human-specific, TranSignal Human Cytokine Array 3.0 (Ray Biotech Inc., Norcross, GA). The antibody array detects granulocyte-macrophage colony-stimulating factor (GM-CSF), interleukin-1α (IL-1α), IL-1β, IL-1 receptor antagonist (IL-1RA), IL-2, IL-3, IL-4, IL-5, IL-6, IL-6R, IL-8, IL-12(p40), IL-15, IL-17, gamma interferon (IFN-γ)-induced protein 10 (IP-10, or CXCL10), matrix metalloproteinase-3 (MMP3), intercellular adhesion molecule 1 (ICAM-1), vascular cell adhesion molecule 1 (VCAM-1), vascular endothelial growth factor (VEGF), macrophage inflammatory protein 1α (MIP-1α, or CCL3), MIP-1β (or CCL4), MIP-4, MIP-5 (or CCL15), Apol/Fas (CD95), cytotoxic T lymphocyte-associated (CTLA), eotaxins, epidermal growth factor (EGF), IFN-γ, monocyte chemoattractant protein 1 (MCP-1, or CCL2), MCP-2, MCP-3, RANTES (regulated on activation normal T cell expressed and secreted, or CCL5), transforming growth factor β1 (TGF-β1), TNF-α, TNF-β, and TNF receptor-1 (TNFR1). Positive responses were further assessed quantitatively by ELISA (Quantikine kits; R&D Systems, Minneapolis, MN). The effects of HIV-1 Tat and/or morphine on TNF-α, IL-6, and RANTES levels were measured by ELISA (Quantikine kits; R&D Systems).

Reactive oxygen species production. Cells were incubated with 10 μM dichlorodihydrofluorescein diacetate (DCFH-DA) (Invitrogen) in warm PBS for 1 h according to the manufacturer's protocol. Dichlorofluorescein (DCF) fluorescence was measured at an excitation wavelength (λ_{ex}) of 485 nm and an emission wavelength (λ_{em}) of 520 nm using a Victor 3 microplate reader (PerkinElmer, Inc., Waltham, MA). ROS levels, estimated by relative DCF fluorescence, were normalized to the proportion of viable cells and reported as DCF mean fluorescence intensity (MFI).

Nitrite assay. Nitrite concentration was determined spectrophotometrically using a modification of the Griess reaction (Griess Reagent System, Promega). The optical density was read at 540 nm.

Nitrotyrosine. 3-Nitrotyrosine levels were quantified by enzyme immunoassay (EIA) using a nitrotyrosine-EIA kit from Oxis International, Inc. (Foster City, CA). Optical density was read at 450 nm.

Measurement of NF-κB activity. DNA-binding activity of NF-κB was measured by an ELISA-based assay using TransAM NF-κB p50 and p65 kits from Active Motif (Carlsbad, CA). Optical density was read at 450 nm.

Western blot analysis. NF-κB activation was confirmed by Western immunoblotting using antibodies against phosphorylated and nonphosphorylated NF-κB p65 and p50 (Table 1). HCV expression was assessed by examining HCV NS3 and core proteins by Western blotting; antibodies against β-actin were used as an internal gel loading control (Table 1).

Cytotoxicity assay. Cell viability was assessed by measurement of released lactate dehydrogenase (LDH), using a CytoTox-96 kit from Promega (Madison, WI). Cell viability was also measured in parallel studies by trypan blue dye exclusion according to the manufacturer's instructions (Invitrogen).

Data analysis. Data were analyzed using analysis of variance (ANOVA) techniques (SYSTAT, version 11.0, for Windows; SYSTAT Inc., Chicago, IL) followed by Duncan's posthoc analyses. An alpha level of $P < 0.05$ was considered significant for all statistical tests used. Data are presented as means ± standard errors of the means (SEM).

RESULTS

HIV-1 Tat and morphine modulate proinflammatory cytokines in Huh-8 cells. Evidence from numerous studies indicates that production of hepatic chemokines could play a role in HCV infection, as well as in HIV-1/HCV coinfection. Increased trafficking of lymphocytes into HCV-infected liver has been observed with chronic disease (52, 71). We initially examined whether cytokine production differed between parental Huh-7 cells and Huh-8 cells containing the subgenomic HCV replicon NS3-NS5B (NS3-5B) (30). Changes in the levels of cytokines and chemokines released in the medium from Huh-7 and Huh-8 cells were evaluated at 24 h (Fig. 1A). Of the 32 chemokines and cytokines screened, the chemokines MIP-1α, MIP-1β, MIP-5, RANTES, and IP-10 and the cytokines TNF-α, IL-1α, IL-4, and IL-12 showed significantly different patterns of release in a comparison of parental Huh-7 (control) and Huh-8 cells, which contain subgenomic HCV (Fig. 1A). Basal levels of secretion for the chemokines/cytokines that responded in Huh-7 cells were as follows (values are in pg/ml): MIP-1α, 3,296.0 ± 95.0; MIP-1β, 557.3 ± 46.7; MIP-5, 3,275.0 ± 562.2; RANTES, 3,855.5 ± 69.9; IP-10, 21,590.3 ± 5,426.8; TNF-α, 237.3 ± 16.2; IL-1α, 123.0 ± 16.9; IL-4, 14,750.0 ± 7,158.2; and IL-12, 32,338.2 ± 6,920.9.

We then examined whether 24-h exposure to HIV-1 Tat and/or morphine would affect cytokine production by HCV replicon-expressing Huh-8 cells (Fig. 1B). $Tat_{1–72}$ alone significantly decreased TNF-α and IL-6 secretion but augmented IL-4 levels while morphine decreased TNF-α and IL-4 secretion but had no effect on IL-6 release (Fig. 1B). The combination of morphine and Tat in HCV-infected cells significantly increased TNF-α and IL-6 levels relative to morphine or Tat alone while IL-4 levels were significantly increased compared to morphine

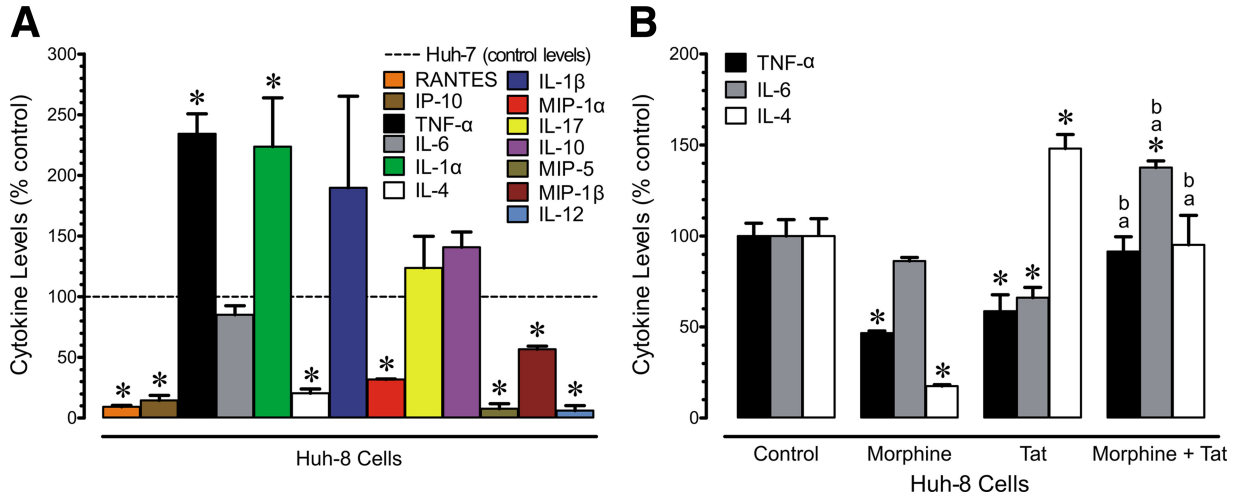

FIG. 1. Altered secretion of proinflammatory cytokines in Huh-8 cells containing a subgenomic HCV replicon. (A) The data show levels of basal secretion of several proinflammatory cytokines in Huh-8 cells relative to the baseline secretion of the same cytokines in parental Huh-7 cells (values represent the percentages of control levels, with the dotted line indicating levels of cytokine secretion in Huh-7 cell controls). Thus, values are the mean change in secreted cytokines in Huh-8 versus Huh-7 cells ± SEM from three independent experiments (*, $P < 0.05$ versus Huh-7 controls). (B) Morphine (500 nM) and/or HIV-1 Tat (100 nM) altered cytokine secretion by Huh-8 cells expressing subgenomic HCV at 24 h following continuous exposure. Values represent the mean ± SEM of three independent experiments (*, $P < 0.05$ versus control; a, $P < 0.05$ versus HIV-1 Tat alone; b, $P < 0.05$ versus morphine alone).

alone but were suppressed compared to Tat alone. Only IL-6 levels were significantly increased relative to HCV infection alone (Fig. 1B). Intrigued by these results, we expanded our observation and included studies using the infectious JFH1 model.

R5- and X4-tropic HIV-1 strains infect Huh7.5.1 cells. To examine the extent to which HIV-1 receptors are present on Huh7.5.1 cells, expression patterns of CD4, CXCR4, and CCR5 on Huh7.5.1 cells were assessed by fluorescence microscopy (Fig. 2A and B), Western immunoblotting (Fig. 2C), and flow cytometry (Fig. 2D). Among Huh7.5.1 cells, flow cytometric determinations demonstrated that 32.2% ± 0.4% were CXCR4 positive, 35.0% ± 2.3% were CCR5 positive (Fig. 2D), and 24.7% ± 0.1% possessed both receptors. CD4 was not detected in Huh7.5.1 cells (data not shown). To determine whether either of these coreceptors mediated infection, we infected Huh7.5.1 cells with HIV-$1_{LAI/IIIB}$ and HIV-1_{SF162}, with and without morphine, in the absence or presence of the CXCR4 antagonist AMD3100 (100 nM) (41, 62) or the CCR5 antagonist maraviroc (100 nM) (44, 62). Infected cells displayed HIV-1 p24 immunoreactivity (Fig. 2E to J), while p24 antigenicity was absent from uninfected cells. Based on the proportion of HIV-1 p24-immunopositive Huh7.5.1 cells, infection with X4 HIV-$1_{LAI/IIIB}$ was inhibited by AMD3100 (Fig. 2K) but not maraviroc (data not shown) while infection with R5 HIV-1_{SF162} was inhibited by maraviroc (Fig. 2L) but not by AMD3100 (data not shown).

Morphine increases R5-tropic, but not X4-tropic, HIV-1 infectivity in Huh7.5.1 cells. Interestingly, exposure to morphine increased the infectivity of R5 HIV-1_{SF162} (Fig. 2L) while X4 HIV-$1_{LAI/IIIB}$ was unaffected by morphine (Fig. 2K). Thus, although the data suggest that HIV-1 can utilize either coreceptor in Huh7.5.1 cells, morphine increased only R5 HIV-1 infectivity under the conditions of the present study.

Although the idea is controversial, numerous groups have shown that HIV-1 can infect cells, including hepatocyte cell lines, via CD4-independent mechanisms (34, 35). In fact, HIV-1 infection in Huh-7 cells has been previously observed (3, 6, 22, 70). To demonstrate HIV-1 infection in Huh7.5.1 cells, we inoculated these cells with X4-tropic HIV-1_{NL4-3} Vpr-GFP and visualized GFP-tagged virions by confocal microscopy (Fig. 3A, HIV-1_{GFP}). Although most cells were not Vpr-GFP positive, hepatic cells possessing internalized Vpr-GFP were clearly evident (Fig. 3A). Next, we examined the presence of HIV-1 Tat in Huh7.5.1 cells using the pBlue3′LTR-luc reporter. Expressed Tat protein levels were 5.2- ± 0.4-fold and 4.4- ± 0.2-fold higher than uninfected background levels in HIV-$1_{LAI/IIIB}$- and HIV-1_{SF162}-infected Huh7.5.1 cells, respectively (Fig. 3B). To further demonstrate HIV-1 infection in Huh7.5.1 cells, RNA from these cells was analyzed by RT-PCR, and an appropriate ~210-bp band corresponding to Tat transcripts was detected in both HIV-1_{NL4-3}- and HIV-1_{BaL}-infected cells but not in uninfected cells (Fig. 3C). Lastly, HIV-1 p24 levels were examined in the medium from HIV-1_{NL4-3} Vpr-GFP-, HIV-$1_{LAI/IIIB}$-, or HIV-1_{SF162}-infected Huh7.5.1 cells by ELISA at 24 h postinoculation (Fig. 3D). HIV-1 p24 was not detectable in uninfected control cells but was readily detectable in HIV-$1_{LAI/IIIB}$, HIV-1_{SF162}, and, to a lesser degree, HIV-1_{NL4-3} Vpr-GFP-infected cells.

HIV-1 increases nitrite production in HCV-infected Huh7.5.1 cells. NO promotes the pathogenesis of numerous viral infections, including hepatitis B and C (15, 17, 24). NO may combine with superoxide anions to form peroxynitrite, which can react with proteins to form damaging 3-NT products (50). NO production was monitored in mock- and JFH1-infected Huh7.5.1 cells incubated with morphine, HIV-1 Tat and gp120, and/or HIV-$1_{LAI/IIIB}$ or HIV-1_{SF162} (Fig. 4A). HCV significantly amplified NO production (0.30 ± 0.2 μM in uninfected versus 1.66 ± 0.3 μM in infected Huh7.5.1 cells), and exposure to gp120 in combination with morphine caused a significant increase in NO production by 1.8- ± 0.1-fold, compared to

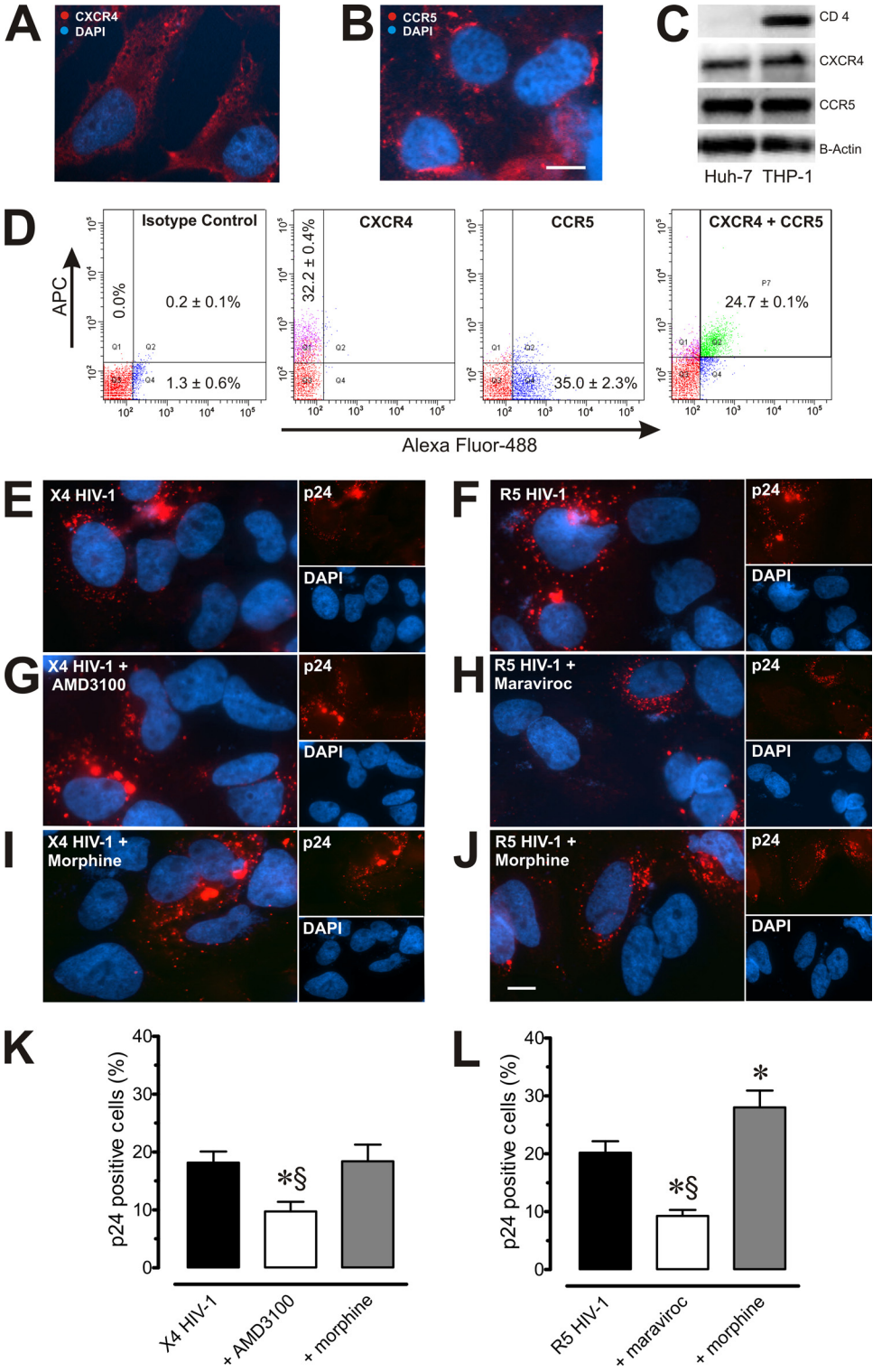

FIG. 2. Expression of CCR5, CXCR4, and HIV-1 infectivity in Huh7.5.1 cells. (A and B) CXCR4 and CCR5 immunofluorescence was detectable in subsets of Huh7.5.1 cells. Scale bar, 10 μm. (C) CXCR4 and CCR5, but not CD4, were readily detectable by Western immunoblotting in Huh7.5.1 cells; CXCR4-, CCR5-, and CD4-coexpressing human acute monocytic leukemia (THP-1) cells served as positive controls. (D) Flow cytometry indicated that about one-third of Huh7.5.1 cells possessed CXCR4 or CCR5 antigenicity, and the receptors colocalized on some cells, as detected by allophycocyanin (APC) or Alexa Fluor 488 fluorescence, respectively. For each cell culture well, 10,000 events were collected, and size discrimination was used as a crude method for viability determination. Values are the mean percentage of immunopositive cells ± SEM from $n = 3$ experiments. (E to L) Uninfected or JFH1-infected Huh7.5.1 cells were preincubated for 30 to 60 min with either the CXCR4 antagonist, AMD3100 (100 nM), or the CCR5 antagonist, maraviroc (100 nM) with or without morphine (500 nM), and infected with HIV-$1_{LAI/IIIB}$ (X4) or HIV-1_{SF162} (R5). After 18 h, cells were rinsed, fixed, and labeled with anti-p24 monoclonal antibodies (red) and counterstained with DAPI (blue). Values are the mean change in percentage of p24-immunopositive cells compared to levels in untreated HIV-1-infected cells (percentage of control) ± SEM from $n = 3$ independent experiments (*, $P < 0.05$ versus HIV-1 alone; §, $P < 0.05$ versus HIV-1 plus morphine).

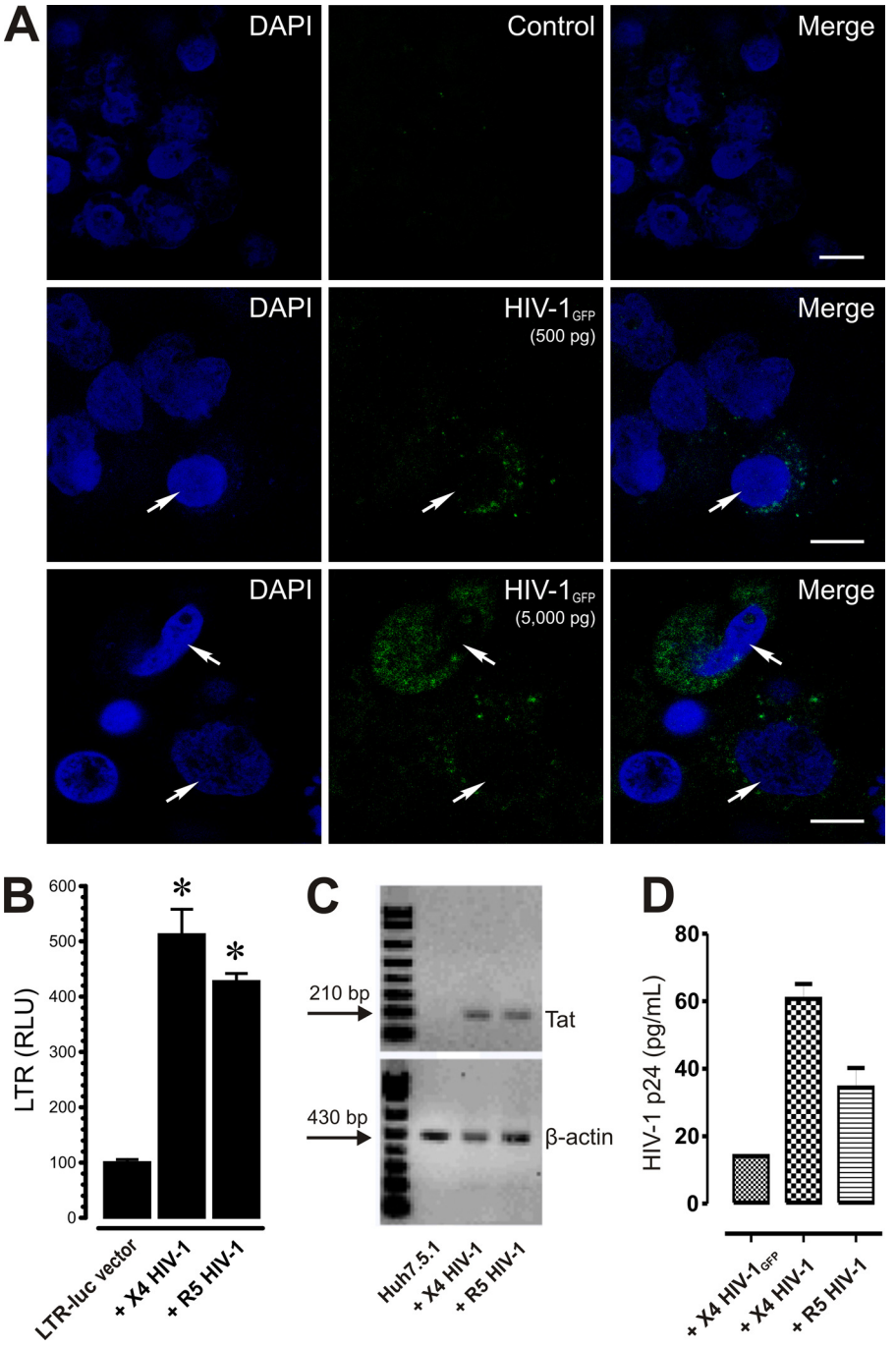

FIG. 3. HIV-1 infection in Huh7.5.1 cells. (A) Cellular localization of HIV-1_{NL4-3}-Vpr-GFP in Huh7.5.1 cells. Huh7.5.1 cells with or without infection with X4-tropic HIV-1_{NL4-3}-Vpr-GFP (HIV-1_{GFP}) reporter virus (green) and counterstained with DAPI (blue) were readily detectable in some cells (arrows) by confocal microscopy. Images are optical sections from a single Z plane with the acquisition parameters set to optimize X-, Y-, and especially Z-plane resolution. Note the relative increases in GFP within infected Huh7.5.1 cells when HIV-1_{GFP} titer is increased from 500 pg/ml p24 (500 pg) to 5,000 pg/ml p24 (5,000 pg), as determined by ELISA. Scale bar, 10 μm. (B) Tat expression in HIV-1-infected Huh7.5.1 cells. Cells were transfected with pBlue3′LTR-luc and inoculated with HIV-$1_{LAI/IIIB}$ (X4) or HIV-1_{SF162} (R5) for 12 h, rinsed three times, and incubated in fresh medium, and Tat protein-driven activation of an LTR-driven, pBlue3′LTR-luc luciferase reporter was measured 48 h postinfection (*, $P < 0.05$ versus uninfected controls). Data are relative luciferase units (RLU) ± SEM from three independent experiments. (C) Tat expression in HIV-1-infected Huh7.5.1 cells. *De novo* HIV-1 Tat transcripts can be detected by RT-PCR in RNA extracted from HIV-1_{NL4-3} (X4)- or HIV-1_{BaL} (R5)-exposed Huh7.5.1 cells. (D) p24 levels in the medium of HIV-1_{GFP}-, HIV-$1_{LAI/IIIB}$ (X4)-, or HIV-1_{SF162} (R5)-infected Huh7.5.1 cells. Huh7.5.1 cells were inoculated with HIV-1 (500 pg/ml p24) and rinsed multiple times, and increases in HIV-1 production were detected by ELISA at 24 h postinfection. Although p24 levels were less in HIV-1_{GFP}-infected cells than in the other HIV-1 strains examined, HIV-1 p24 was not detectable in uninfected control cells (data not shown). Data are mean HIV-1 p24 (pg/ml) ± SEM from at least three separate determinations.

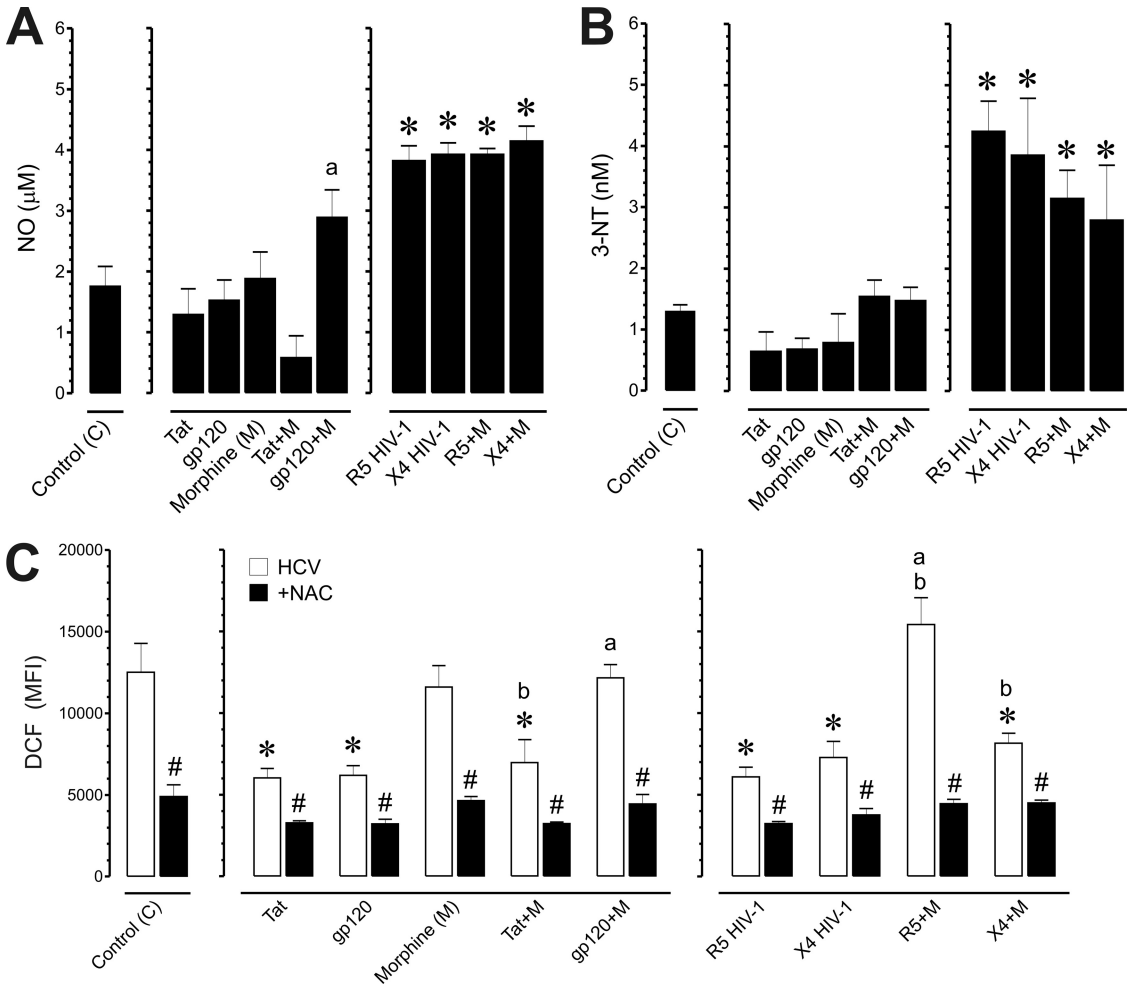

FIG. 4. Effects of HIV-1 and/or morphine on the production of NO and 3-nitrotyrosine (3-NT) products in HCV-infected Huh7.5.1 cells. HCV (JFH1)-infected Huh7.5.1 cells were treated with HIV-1 Tat (100 nM), bitropic $gp120_{MN}$ (500 pM), X4-tropic $HIV\text{-}1_{LAI/IIIB}$, or R5-tropic $HIV\text{-}1_{SF162}$ with or without morphine (500 nM) and assessed at 24 h following treatment. (A) HIV-1 infection significantly increased NO levels in HCV-infected cells (*, $P < 0.05$ versus control) while exposure to HIV-1 proteins did not increase NO. The effect of combined gp120 with morphine was significantly greater than that of gp120 alone (a, $P < 0.05$ versus gp120) but was not increased above HCV-infected cells without supplemental treatments. NO levels were estimated by examining nitrite concentration. Values are the mean ± SEM from three independent experiments. (B) 3-NT products were significantly increased by $HIV\text{-}1_{LAI/IIIB}$ or R5-tropic $HIV\text{-}1_{SF162}$ in HCV-coinfected Huh7.5.1 cells irrespective of morphine treatment (*, $P < 0.05$ versus control) while morphine and/or HIV-1 proteins had no effect on 3-NT levels. 3-NT levels were assayed by ELISA; values are the mean 3-NT concentration (nM) ± SEM from four independent experiments. (C) ROS production in HCV-infected Huh7.5.1 cells. HCV (JFH1)-infected Huh7.5.1 cells were pretreated with NAC (10 μM) followed by incubation with HIV-1 Tat (100 nM), bitropic $gp120_{MN}$ (500 pM), X4-tropic $HIV\text{-}1_{LAI/IIIB}$, or R5-tropic $HIV\text{-}1_{SF162}$ with or without morphine (M) (500 nM) and assessed at 24 h postinfection. ROS was subsequently assessed by DCF fluorescence. Values are DCF mean fluorescence intensity (MFI) ± SEM of three independent experiments at 24 h postinfection (*, $P < 0.05$ versus control; a, $P < 0.05$ versus HIV-1 protein or HIV-1 isolate alone; b, $P < 0.05$ versus morphine alone; #, $P < 0.05$ versus HCV JFH1 without NAC).

gp120 alone, while combined Tat and morphine treatment trended toward a decrease in NO production but was not significant. Both $HIV\text{-}1_{LAI/IIIB}$ and $HIV\text{-}1_{SF162}$ alone significantly enhanced NO production by about 2-fold in JFH1 HCV-coinfected Huh7.5.1 cells while morphine caused no additional increases in NO production in the coinfected cells (Fig. 4A). The results show that HCV infection increased the production of nitrites in Huh7.5.1 cells (data not shown) while combined HCV and HIV-1 exposure typically enhanced the response by about 2-fold. Morphine had no additional effect in coexposed hepatocytes. Next, we examined the effects of HCV on 3-NT production, a relatively selective marker of nitrosative damage by peroxynitrite (50). HCV increased 3-NT products (0.42 ± 0.06 nM in uninfected versus 1.18 ± 0.07 nM in infected Huh7.5.1 cells); however, unlike the approximate 2-fold increases in NO, exposure to HIV-1 Tat or gp120 had no additional effect on 3-NT compared to HCV infection alone (Fig. 4B). On the contrary, coinfection with $HIV\text{-}1_{LAI/IIIB}$ or $HIV\text{-}1_{SF162}$ significantly enhanced 3-NT production by 2.6- ± 0.2-fold and 3.3- ± 0.2-fold, respectively, while concurrent morphine exposure had no interactive effect (Fig. 4B).

HIV-1 suppresses ROS production in HCV-infected cells, while morphine negates many of the suppressive effects of HIV-1. Our results corroborate prior findings that HCV in-

fection increases ROS (31) but differ from a report that HCV and HIV-1 coinfection cooperatively increases ROS (33). Although HCV infection significantly induced ROS production in Huh7.5.1 cells compared to uninfected controls (2.69- ± 0.2-fold increase), coexposure to Tat or gp120, or coinfection with HIV-$1_{LAI/IIIB}$ or HIV-1_{SF162} significantly decreased oxyradical levels by about 2-fold compared to HCV infection alone (Fig. 4C). Exposing HCV-infected cells to morphine alone had no effect on ROS; however, in combination with dual-tropic $gp120_{MN}$ or R5-tropic HIV-1_{SF162}, morphine prevented HIV-1 from restricting ROS production ($P < 0.05$) (Fig. 4C, gp120+M and R5+M). Interestingly, morphine did not prevent the reduction in ROS in X4-tropic HIV-$1_{LAI/IIIB}$-coinfected cells (Fig. 4C). Together with findings examining HIV-1 infectivity (Fig. 2), the ROS data suggest that morphine selectively affects CCR5 but not CXCR4 interactions with HIV-1 in HCV/HIV-1-coinfected hepatic cells. Lastly, treatment with the antioxidant NAC significantly attenuated ROS production across all treatments ($P < 0.05$) (Fig. 4C, filled bars).

HIV-1 and morphine cooperatively increase TNF-α and CCL5/RANTES secretion in HCV JFH1-infected cells. The effects of HIV-1 and morphine on the release of proinflammatory cytokines by uninfected and HCV (JFH1)-infected cells were examined. TNF-α, IL-6, and CCL5/RANTES levels were 32.3 ± 24.0 pg/ml, 17.8 ± 2.6 pg/ml, and 3.9 ± 1.9 pg/ml, respectively, in untreated, mock HCV-infected Huh7.5.1 cells at 8 h. Interestingly, in untreated, HCV-infected Huh7.5.1 cells, TNF-α, IL-6, and CCL5/RANTES levels were 92.3 ± 2.0 pg/ml, 26.7 ± 5.1 pg/ml, and 7.3 ± 3.0 pg/ml, respectively, at 8 h (Fig. 5A to C), which did not differ from native levels in Huh7.5.1 cells. Cytokine levels in HIV-1-infected and/or morphine-treated HCV (JFH1)-infected Huh7.5.1 cells were compared to values in untreated, HCV (JFH1)-infected Huh7.5.1 cells (Fig. 5). HIV-1 altered the production of TNF-α and IL-6, with exposure to gp120 significantly increasing TNF-α production by 1.62 ± 0.12-fold (Fig. 5A) and significantly decreasing IL-6 levels by 1.31 ± 0.08-fold at 8 h following treatment (Fig. 5B). Alternatively, combined gp120 and morphine treatment significantly increased RANTES production compared to levels in controls or with gp120 alone after 8 h (Fig. 5C). Exposure to Tat produced minimal interactions with HCV while morphine plus Tat together caused a marked increase in TNF-α production at 8 h and 24 h. After 72 h, the response to the viral proteins was largely gone.

Proteasome inhibition reduces the inflammatory response while NAC increases oxyradical production in response to some treatments. Viruses belonging to several different families have been shown to utilize or modulate the ubiquitin-protease system to their advantage during their infection cycles (25, 47, 49). To provide molecular insight into how HIV-1 and morphine might exert their proinflammatory effects on HCV-infected hepatocytes, we examined whether the ubiquitin-proteasome system is involved by using a selective proteasome inhibitor, MG132 (Fig. 5). We focused on morphine's interactions with R5-tropic HIV-1 in this experiment since the X4 (LAI/IIIB) strain showed fewer interactions with morphine (Fig. 2K and L and 4C; also unpublished observations). Treatment with MG132 significantly attenuated cytokine production in HCV-infected Huh7.5.1 cells (Fig. 5A to C). We also tested whether ROS production triggers the cytokine release accompanying HCV infection in hepatocytes. The antioxidant NAC failed to negate HCV-induced increases in TNF-α, IL-6, and RANTES production (Fig. 5A to C); instead, NAC caused additive increases in cytokine release in some instances with the most noticeable boost in RANTES secretion (Fig. 5C).

Compared to HCV infection alone, coinfection with HIV-1_{SF162} had no additional effects on TNF-α release (Fig. 6A); however, IL-6 was decreased (Fig. 6A) while RANTES levels significantly increased (Fig. 6A), depending on viral concentration. Combined exposure to HIV-1_{SF162} (p24 titer, 5,000 pg/ml) with morphine tended to increase TNF-α levels, albeit not significantly ($P \leq 0.06$), while RANTES production was markedly augmented with exposure to 5,000 pg of HIV-1_{SF162} alone. Greater virus-virus interactions were seen when a chronic, steady-state infection was established after 72 h, and for this reason, only data at 72 h are shown. We confirmed that HCV infection did not increase TNF-α, IL-6, and RANTES production (data not shown) while coexposure with HIV-1_{SF162} with or without morphine significantly increased TNF-α and RANTES production. Importantly, the data also show that coexposure to HCV, HIV-1, and morphine can create dramatic imbalances in the hepatic inflammatory response.

To explore how the above manipulations affected NF-κB activation, phosphorylated and total levels of the p50 and p65 NF-κB subunits were analyzed by Western immunoblotting (Fig. 6B and C). Neither HIV-1 Tat, gp120, nor morphine alone had any effect on p65 phosphorylation (P~p65) in HCV-infected Huh7.5.1 cells (Fig. 6B and C). In contrast, combined morphine plus gp120 or morphine plus HIV-1 Tat significantly elevated P~p65 (Fig. 6B and C). With MG132 pretreatment, the levels of P~p65 were significantly reduced (Fig. 6B and C). Unlike the p65 subunit, neither p50 (including p50 monomers and p50 dimers) nor phosphorylated p50 (P~p50) levels were affected by exposure to HIV-1 Tat, gp120, and/or morphine, or by MG132 (Fig. 6C).

To determine whether the ubiquitin-proteasome system is involved in HCV propagation, HCV infection was monitored by measuring NS3 and HCV core levels (Fig. 7A and B). HCV NS3 and core protein levels were significantly increased after exposure to Tat or gp120 while exposure to morphine alone had no effect on HCV NS3 or core protein values. Interestingly, concurrent morphine exposure prevented HIV-1 Tat or gp120-induced increases in amounts of HCV NS3 or core proteins and, in some cases, significantly abrogated Tat- or gp120-induced increases in HCV protein levels. Contrary to the prevailing sentiment that antioxidants are beneficial, exposure to NAC alone caused significant increases in HCV core protein values in HCV JFH1-infected cells (Fig. 7B) and failed to counter increases in NS3 protein levels caused by HIV-1 Tat or gp120 (Fig. 7A). Inhibition of proteasome function significantly reduced HCV NS3 and core protein levels and blocked both HIV-1 Tat- and gp120-induced increases in HCV NS3 and core proteins in HCV-infected hepatocytes (Fig. 7). The results show that inhibition of the ubiquitin-proteasome system reduces viral protein levels, coinciding with attenuated release of proinflammatory cytokines and NF-κB activation. Alternatively, NAC-dependent reductions in ROS and concomitant increases in HCV viral proteins suggest that the innate host

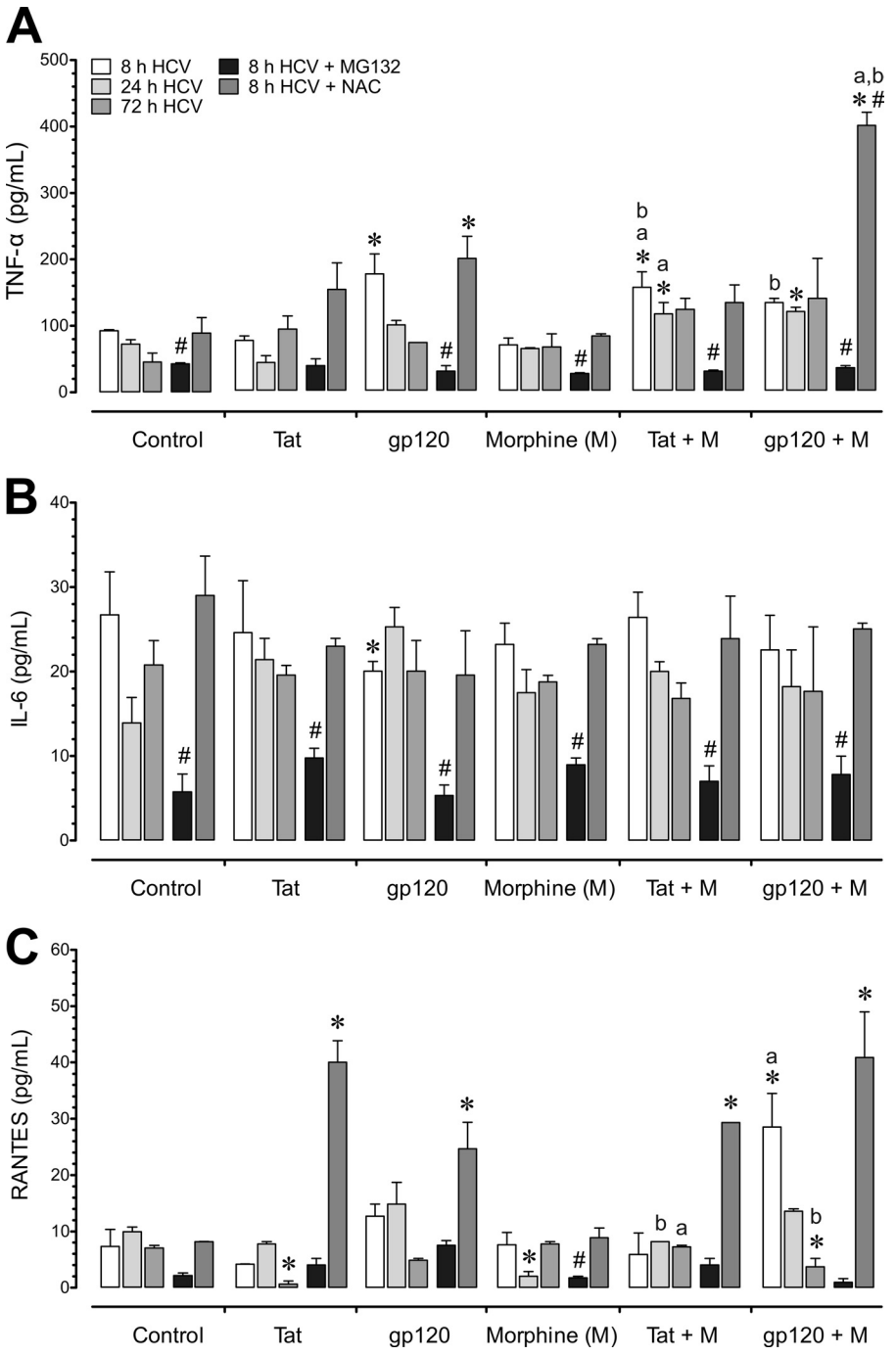

FIG. 5. Effects of HIV-1, morphine, and/or a proteasome inhibitor or a free radical scavenger on the release of proinflammatory cytokines from HCV-infected Huh7.5.1 cells. HCV (JFH1)-infected Huh7.5.1 cells were pretreated with the proteasome inhibitor MG132 (10 μM) or the ROS inhibitor *N*-acetyl cysteine (NAC) (10 μM), followed by incubation with HIV-1 Tat (100 nM) or bitropic $gp120_{MN}$ (500 pM) with or without morphine (M) (500 nM) and assessed at 8 h, 24 h, and 72 h following treatment. (A) TNF-α levels were significantly increased with gp120 alone at 8 h and enhanced to a lesser extent when gp120 was coadministered with morphine at 24 h, as well as with combined Tat and morphine (M) exposure at 8 h and 24 h. (B) IL-6 was significantly decreased after 8 h exposure to gp120 but was otherwise unaffected by HIV-1 protein or morphine exposure. MG132 attenuated IL-6 secretion at 8 h and showed sustained reductions at 24 h and 72 h (data not shown). (C) RANTES showed a transient increase in release with combined gp120 and morphine at 8 h, followed by marked decline when the same treatment was sustained for 72 h. Morphine and Tat alone caused significant declines in RANTES at 24 h and 72 h, respectively. Unlike TNF-α and IL-6, MG132 treatment did not reduce RANTES levels below those seen in untreated, HCV-infected cells, with the exception of a marked decline following 8 h of morphine exposure. In the presence of NAC, HIV-1 proteins markedly increased RANTES release irrespective of whether morphine was coadministered while morphine alone had no affect on RANTES production. Values represent the mean ± SEM from three independent experiments (*, $P < 0.05$ versus untreated, HCV-infected controls; a, $P < 0.05$ versus HIV-1 protein alone; b, $P < 0.05$ versus morphine alone; #, $P < 0.05$ versus HCV-infected group without inhibitor).

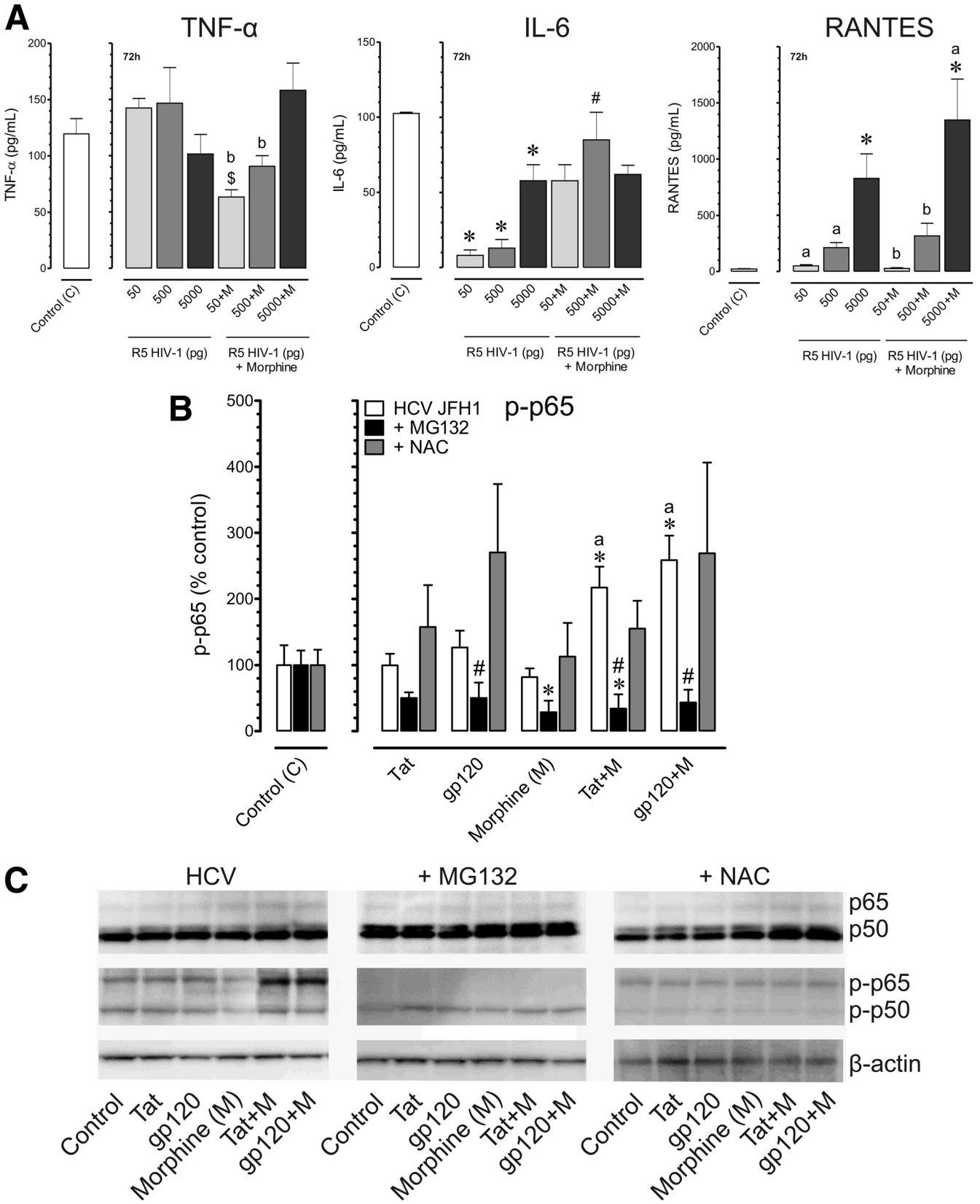

FIG. 6. Effects of inhibiting proteasome function or a ROS scavenger on the inflammatory response to HCV and HIV-1 coinfection with or without morphine. HCV (JFH1)-infected Huh7.5.1 cells were pretreated with MG132 (10 μM) or the ROS scavenger *N*-acetyl cysteine (NAC) (10 μM), followed by incubation with HIV-1 Tat (100 nM) or bitropic $gp120_{MN}$ (500 pM) with or without morphine (M) (500 nM) and assessed at 8 h following treatment. (A) HCV-infected Huh7.5.1 cells were inoculated with R5-tropic HIV-1_{SF162} at concentrations of 50,500, or 5,000 pg/ml

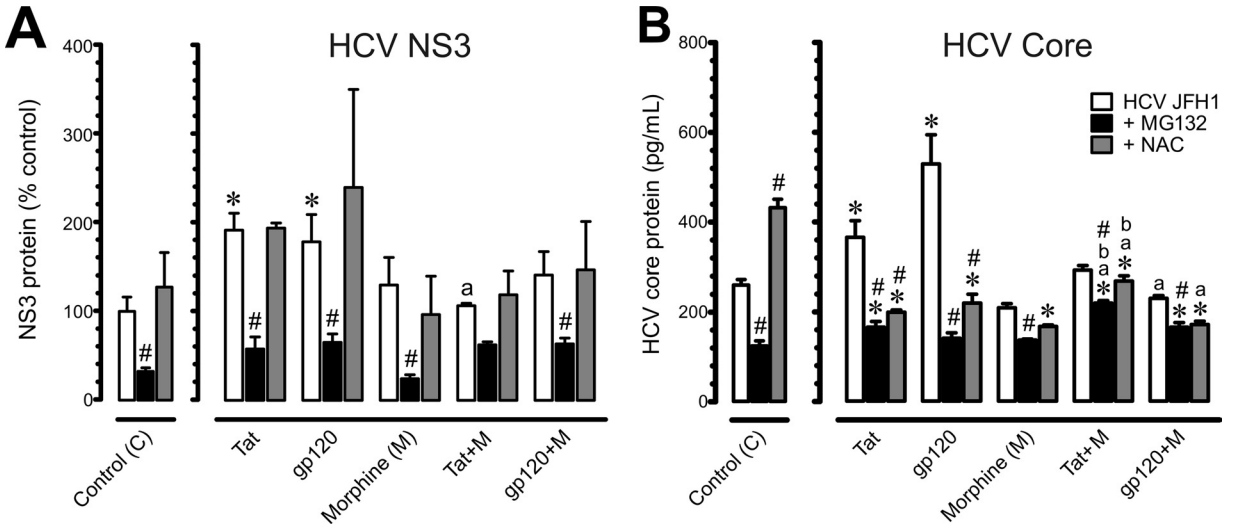

FIG. 7. Effects of HIV-1 proteins and/or morphine on HCV NS3 and core protein levels in HCV JFH1-infected Huh7.5.1 cells at 8 h following exposure. HCV (JFH1)-infected Huh7.5.1 cells were pretreated with the proteasome inhibitor MG132 (10 μM) or the ROS inhibitor *N*-acetyl cysteine (NAC) (10 μM), followed by incubation with HIV-1 Tat (100 nM) or bitropic $gp120_{MN}$ (500 pM) with or without morphine (M) (500 nM) and assessed at 8 h following treatment. (A) HCV NS3 protein was assayed by Western blot analysis and normalized to β-actin. Data are mean change in NS3 protein levels relative to HCV infection alone (percentage of control) ± SEM from three independent experiments (∗, $P < 0.05$ versus control; a, $P < 0.05$ versus HIV-1 alone; #, $P < 0.05$ versus HCV JFH1 without inhibitor). (B) HCV core levels were assayed by ELISA. Values are mean HCV core protein levels (pg/ml) ± SEM from three independent experiments (∗, $P < 0.05$ versus untreated, HCV-infected controls; a, $P < 0.05$ versus HIV-1 protein alone; b, $P < 0.05$ versus morphine alone; #, $P < 0.05$ versus HCV-infected controls without inhibitor).

defense-mediated increase in ROS is advantageous in limiting HCV expression.

The experimental treatments did not affect Huh7.5.1 cell viability. To determine whether HIV-1 Tat, gp120, and/or morphine exposure affected Huh7.5.1 cell viability in the presence or absence of MG132 or NAC, both LDH (Fig. 8) and trypan blue dye exclusion (data not shown) assays were performed at 48 h. HIV-1 Tat, gp120, and/or morphine with or without NAC or MG132 did not significantly affect the survival of HCV JFH1-infected hepatic cells.

DISCUSSION

In this study, we explored HCV–HIV-1 interactions and the superimposition of the opiate drug morphine on host immune responses, including the production of free radicals and proinflammatory cytokines. While production of reactive nitrogen and oxygen species (RNS and ROS, respectively) is a component of innate defense against viral infection, their overproduction can be deleterious. Moreover, although morphine can alter HIV-1 entry into brain cells (19, 36, 39, 54), less is known about its effects in mono-infected or HCV- and HIV-1 coinfected hepatocytes. Using hepatocytes and *in vitro* replication models of HCV, we present the following evidence: (i) that HCV induced the production of ROS, NO, and 3-NT and the proinflammatory cytokines TNF-α, IL-6, and, to a lesser extent, RANTES; (ii) that HIV-1 entered Huh7.5.1 cells via the HIV-1 coreceptors, CXCR4 and CCR5, in a CD4-independent manner, and coexposure with HIV-1 caused significant increases in HCV-induced oxyradical production and proinflammatory cytokine release; (iii) that morphine increased HIV-1 infectivity, and in combination with HIV-1 and HCV, morphine further enhanced virally induced inflammatory responses; and (iv) that the antioxidant NAC was effective in reversing ROS induction but was unable to attenuate HCV protein levels or virally induced cytokine release, while inhibiting the ubiquitin-proteasome system significantly attenuated viral protein production and host cytokine release. The last finding suggests that alterations in HCV pathogenesis are mediated by the host proteasome system through actions involving NF-κB.

While we find some hepatic cells are infected with HIV-1, many of the responses evoked by HIV-1 in liver parenchyma may be bystander effects (40, 68). The present study did not determine whether the infection with both viruses is in the

alone and in combination with morphine (500 nM) for 72 h. Values represent mean cytokine levels ± SEM of three independent experiments (∗, $P < 0.05$ versus control; $, $P < 0.05$ versus HIV-1 50 pg; #, $P < 0.05$ versus HIV-1 500 pg; a, $P < 0.05$ versus HIV-1 5000 pg; b, $P < 0.05$ versus HIV-1 with 5,000 pg of morphine). (B) Phosphorylation of the p65 (P~p65) subunit of NF-κB was monitored by Western blot analysis, normalized to total p65, and compared to untreated HCV JFH1-infected cells. Values are the mean ± SEM from three independent experiments (∗, $P < 0.05$ versus untreated, HCV-infected controls; a, $P < 0.05$ versus HIV-1 protein alone; #, $P < 0.05$ versus HCV-infected group without inhibitor). (C) Combined HIV-1 proteins with morphine increase P~p65 levels while neither HIV-1 proteins nor morphine alone affects p65 phosphorylation. MG132 dramatically attenuated P~p65 while NAC caused a relative decline in p50 levels in Western immunoblots of p50 and p65 and their phosphorylated counterparts, P~p50 and P~p65, respectively.

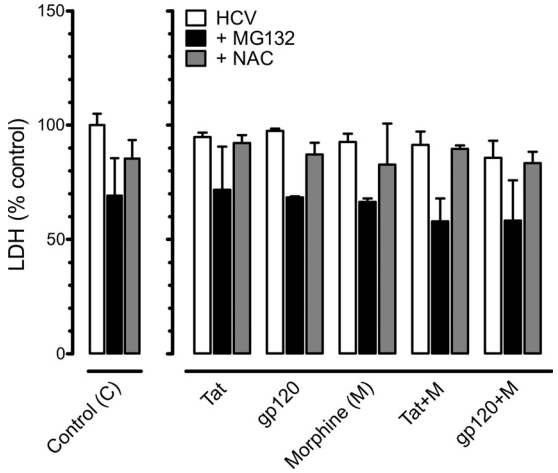

FIG. 8. HIV-1 proteins and/or morphine did not affect the viability of HCV-infected Huh7.5.1 cells irrespective of pretreatment with a proteasome inhibitor or a free radical scavenger. HCV-infected Huh7.5.1 cells were pretreated with the proteasome inhibitor MG132 (10 μM) or the ROS inhibitor *N*-acetyl cysteine (NAC) (10 μM) and incubated with HIV-1 Tat (100 nM) or bitropic $gp120_{MN}$ (500 pM) with or without morphine (M) (500 nM). Cell viability, assessed by lactate dehydrogenase (LDH) levels, was unaffected by HIV-1 proteins and/or morphine at 48 h following continuous exposure. Data are mean LDH levels (percentage of untreated, HCV-infected control cells) ± SEM from three independent experiments.

same cell, different cells, or both. In fact, coinfection increases apoptotic death in Huh7.5.1 cells (23), suggesting that coinfected cells are short-lived. Moreover, the extent to which coinfection in Huh7.5.1 hepatic cells, under artificial conditions, translates into cytopathic changes in human liver disease is uncertain. Though an appreciation of the cell and molecular responses of coinfected hepatocytes is fundamental toward understanding cellular pathogenesis, understanding the coordinated histopathologic response to dual infection is essential for managing the comorbidity therapeutically. As in the brain, we speculate that the collective hepatocyte inflammatory response to HIV-1 originates from a small percentage of infected macrophages/Kupffer cells and perhaps a smaller proportion of hepatocytes but is amplified by reverberant inflammatory responses of large numbers of uninfected macrophages and hepatocytes through paracrine and autocrine feedback.

In Huh-8 hepatoma cells containing a subgenomic HCV replicon, morphine was previously shown to increase the expression of HCV transcripts (30). Furthermore, morphine withdrawal was found to exacerbate HCV replicon expression above levels seen with morphine alone, suggesting complex relationships between opiate drug exposure and HCV replication (66). Morphine is also reported to facilitate HCV replication in human hepatocytes by inhibiting intrahepatic alpha interferon (IFN-α) expression (29). Not only does heroin and morphine metabolism tax hepatocyte resources, but opioid receptors, including the μ-opioid receptor, are also widely distributed on lymphocytes, macrophages (including Kupffer cells [42]), and hepatocytes, indicating that opioids can affect hepatic signaling (68). Thus, opiates have the potential to directly regulate opioid receptor expression on the hepatocytes themselves (4, 69). The μ-opioid receptor, CCR5, and CXCR4 are G-protein-coupled receptors (GPCRs) (11, 26); they can undergo heterologous cross-desensitization and may even interact directly at the molecular level to form heterodimers (11, 26). Thus, exposure to opioids may affect a variety of functions in liver, including hepatocyte metabolism and function, while modifying immune-hepatocyte interactions, such as inhibiting cellular immune responses, modifying chemotactic responses of immune cells (37, 55, 57), and inducing the expression of CCR5 receptors on immunocytes or hepatocytes (39).

Our results corroborate the findings of other investigators that human hepatocytes and hepatocytic cell lines can be infected with HIV-1 (3, 6, 22, 70). In contrast, some human hepatoma cell lines lack both CD4 and CXCR4 at the cell surface and are not productively infected with X4-tropic HIV-1 strains (16). This discrepancy could relate to methodological differences used to detect cell surface receptors or the loss of or altered HIV-1 coreceptor expression due to multiple passages of the cell lines. Our studies included the necessary controls, such as the HIV-1 entry inhibitors maraviroc and AMD3100, to permit discrimination between *de novo* viral particle production and viral recycling. Furthermore, recent studies by Lin and coworkers examined direct virus-virus interactions and showed that X4- and R5-tropic HIV-1 strains can infect Huh7.5.1 cells and, additionally, demonstrated that HIV-1 or HIV-1 proteins can enhance HCV JFH1 replication (23, 32, 33). In the present study, HCV infection significantly increased ROS and RNS, and these reactive products were further elevated by exposure to HIV-1 proteins or by coinfection with HIV-1. This substantiates the findings of other investigators that HCV, as well as HCV core, NS3, and NS5 proteins, increases ROS production, which may contribute to increases in viral replication (12, 38). The expression of TNF-α and its cognate receptors increases in various models of inflammatory liver injury, including HCV infection, presumably as part of innate immune defenses (20, 27, 74). However, coinfection with HIV-1 caused a decrease in HCV-induced IL-6 production, suggesting that in cases where infection with both viruses intensifies TNF-α and RANTES release, HIV-1 can exert an additional role by suppressing some aspects of immune function in an attempt to protect itself from host challenges while exacerbating the infection.

Interestingly, morphine alone minimally affected the cellular response to HCV; however, in combination with HIV-1 proteins or R5-tropic $HIV\text{-}1_{SF162}$ isolates, morphine significantly increased RANTES. Although RANTES has been shown to suppress R5 HIV-1 entry and replication *in vitro*, RANTES has competing roles in the nervous system, where it has been demonstrated to recruit inflammatory macrophages and escalate reactive gliosis in an experimental model of HIV-1 encephalitis (14). Moreover, at high concentrations, RANTES was shown to both activate the host immune response and enhance HIV-1 infection *in vitro* (2). In fact, overexpression of RANTES reportedly exacerbates rabies virus pathogenicity by causing a persistent high level of expression of other chemokines, excessive infiltration, and accumulation of inflammatory cells in the nervous system and augmenting blood-brain barrier permeability (73). This suggests that overexpression of some chemokines such as RANTES, although potentially important in controlling viral infection, may not always be beneficial to the host. In fact, we propose that the imbalances in homeo-

static, host defense responses created by multiple infections and compounded by injection drug use are sufficiently complex that it is not feasible to predict whether the increases or decreases in a particular cytokine described in the present study are beneficial or detrimental without additional experiments.

Collectively, the results indicate that NF-κB regulates HIV-1 Tat, gp120, and/or morphine-induced inflammation and HCV expression and suggests that phosphorylation of p65 mediates key aspects of the exacerbated pathology caused by opiate exposure in HCV- and HIV-1-coinfected liver cells. Blocking proteasome function, which prevents NF-κB activation by impeding dissociation of IκBα from NF-κB p65/p50 subunit complexes, provided additional support for NF-κB and p65 involvement. Thus, HIV-1 proteins alone or in combination with morphine preferentially target the p65 subunit of the transcription factor, leading to the activation of cytokines and chemokines through modification of this protein in hepatocytes. Interestingly, a potent antioxidant, NAC, exacerbated the release of inflammatory cytokines. We speculate that HCV hijacks the cell, and the normal hepatic response to ROS, which typically signals inflammation, is overridden. Accompanying the increases in cytokine production with NAC exposure, there were reductions in p65 phosphorylation compared to controls (Fig. 6D and E).

Indeed, few studies thus far have examined virus-virus interactions in combination with opiate drug abuse because of the inherent complexities of modeling each disease. However, despite the complexity of the interactions, the present study reveals some potential common sites of HCV, HIV-1, and opiate convergence that might be targeted therapeutically. For example, our findings indicate that inhibiting the proteasome markedly reduced TNF-α and RANTES release and decreased HCV NS3 protein levels, irrespective of viral and/or morphine insults, while inhibiting ROS could paradoxically increase the production of some cytokines while decreasing HCV core protein levels. Further studies are needed to elucidate whether the decreased viral protein levels correlate with inhibition of HCV since proteasome inhibitors can have complex effects on HCV pathogenesis (46). Understanding how opioids exacerbate the pathology and complications of HIV-1 and HCV coexposure by temporally distorting the production of proinflammatory cytokines or by sustaining or desynchronizing anti-HCV factors should improve our knowledge and ability to treat current and recovering HCV-infected and, especially, HCV/HIV-1-coinfected IDUs.

ACKNOWLEDGMENTS

We are grateful to these investigators and institutes for supplying the reagents listed here: Takaji Wakita (National Institute for Infectious Diseases, Tokyo, Japan) for the HCV JFH1 constructs; Francis V. Chisari and Stefan Wieland (The Scripps Research Institute, La Jolla, CA) for the Huh7.5.1 cell line and technical advice; Wen-Zhe Ho (Temple University, Philadelphia, PA) for Huh-8 cells, Fatah Kashanchi (George Mason University, Manassas, VA) for the X4 HIV-1_{NL4-3} strain; Avindra Nath (NINDS, Bethesda, MD) and Philip Ray (University of Kentucky, Lexington, KY) for providing HIV-1 Tat; and Yan Zhang (Virginia Commonwealth University) for kindly providing maraviroc. We thank Pamela E. Knapp (Virginia Commonwealth University) for helpful suggestions and editing the manuscript.

Flow cytometry was supported, in part, by NIH National Cancer Institute Cancer Center Support Grant P30 CA016059. This project was funded by NIH National Institute on Drug Abuse (NIDA) grants DA026744 (N.E.-H.), DA019398 (K.F.H.), and DA027374 (K.F.H.).

We do not have a commercial or other association that might pose a conflict of interest.

REFERENCES

1. **Alter, M. J.** 2007. Epidemiology of hepatitis C virus infection. World J. Gastroenterol. **13:**2436–2441.
2. **Appay, V., et al.** 2000. RANTES activates antigen-specific cytotoxic T lymphocytes in a mitogen-like manner through cell surface aggregation. Int. Immunol. **12:**1173–1182.
3. **Banerjee, R., K. Sperber, T. Pizzella, and L. Mayer.** 1992. Inhibition of HIV-1 productive infection in hepatoblastoma HepG2 cells by recombinant tumor necrosis factor-alpha. AIDS **6:**1127–1131.
4. **Bergasa, N. V., and V. D. Boyella.** 2008. Liver derived endogenous opioids may interfere with the therapeutic effect of interferon in chronic hepatitis. Med. Hypotheses **70:**556–559.
5. **Bruno, R., et al.** 2010. Gp120 modulates the biology of human hepatic stellate cells: a link between HIV infection and liver fibrogenesis. Gut **59:** 513–520.
6. **Cao, Y. Z., et al.** 1990. CD4-independent, productive human immunodeficiency virus type 1infection of hepatoma cell lines in vitro. J. Virol. **64:**2553–2559.
7. **Castera, L., et al.** 2005. Hepatitis C virus-induced hepatocellular steatosis. Am. J. Gastroenterol. **100:**711–715.
8. **Cerny, A., and F. V. Chisari.** 1999. Pathogenesis of chronic hepatitis C: immunological features of hepatic injury and viral persistence. Hepatology **30:**595–601.
9. **Cheng-Mayer, C., and J. A. Levy.** 1988. Distinct biological and serological properties of human immunodeficiency viruses from the brain. Ann. Neurol. **23:**S58–S61.
10. **Choi, J., and J-H.Ou.** 2006. Mechanisms of liver injury. Oxidative stress in the pathogenesis of hepatitis C virus. Am. J. Physiol. Gastrointest. Liver Physiol. **290:**G847–G851.
11. **Devi, L. A.** 2001. Heterodimerization of G-protein-coupled receptors: pharmacology, signaling and trafficking. Trends Pharmacol. Sci. **22:**532–537.
12. **Dionisio, N., et al.** 2009. Hepatitis C virus NS5A and core proteins induce oxidative stress-mediated calcium signaling alterations in hepatocytes. J. Hepatol. **50:**872–882.
13. **Duggan, S. T., L. J. Scott.** 2010. Morphine/naltrexone. CNS Drugs **24:**527–538.
14. **El-Hage, N., et al.** 2008. Morphine exacerbates HIV-1 Tat-induced cytokine production in astrocytes through convergent effects on [Ca(2+)](i), NF-κB trafficking and transcription. PLoS One **3:**e4093.
15. **Eum, H. A., S. W. Park, and S. M. Lee.** 2007. Role of nitric oxide in the expression of hepatic vascular stress genes in response to sepsis. Nitric Oxide **17:**126–133.
16. **Fromentin, R., M. R. Tardif, and M. J. Tremblay.** 2011. Inefficient fusion due to a lack of attachment receptor/co-receptor restricts productive human immunodeficiency virus type 1 infection in human hepatoma Huh7.5 cells. J. Gen. Virol. **92:**587–597.
17. **Grattagliano, I., et al.** 2008. Severe liver steatosis correlates with nitrosative and oxidative stress in rats. Eur. J. Clin. Invest. **38:**523–530.
18. **Guidotti, L. G., F. V. Chisari.** 2006. Immunobiology and pathogenesis of viral hepatitis. Annu. Rev. Pathol. **1:**23–61.
19. **Guo, C. J., et al.** 2002. Morphine enhances HIV infection of human blood mononuclear phagocytes through modulation of beta-chemokines and CCR5 receptor. J. Investig. Med. **50:**435–442.
20. **Hatano, E.** 2007. Tumor necrosis factor signaling in hepatocyte apoptosis. J. Gastroenterol. Hepatol. **22:**S43–S44.
21. **Hsiao, P. N., et al.** 2009. Morphine induces apoptosis of human endothelial cells through nitric oxide and reactive oxygen species pathways. Toxicology **256:**83–91.
22. **Iser, D. M., et al.** 2010. Coinfection of hepatic cell lines with human immunodeficiency virus and hepatitis B virus leads to an increase in intracellular hepatitis surface antigen. J. Virol. **84:**5860–5867.
23. **Jang, J. Y., et al.** 2011. HIV infection increases HCV-induced hepatocyte apoptosis. J. Hepatol. **54:**612–620.
24. **Kandemir, O., A. Polat, and A. Kaya.** 2002. Inducible nitric oxide synthase expression in chronic viral hepatitis and its relation with histological severity of disease. J. Viral. Hepat. **9:**419–423.
25. **Katsuma, S., A. Tsuchida, N. Matsuda-Imai, W. Kang, and T. Shimada.** 2011. Role of the ubiquitin-proteasome system in Bombyx mori nucleopolyhedrovirus infection. J. Gen. Virol. **92**(Pt 3)**:**699–705.
26. **Kieffer, B. L.** 1995. Recent advances in molecular recognition and signal transduction of active peptides: receptors for opioid peptides. Cell. Mol. Neurobiol. **15:**615–635.
27. **Kuhla, A., et al.** 2008. Hepatocellular apoptosis is mediated by TNF alpha-dependent Fas/FasLigand cytotoxicity in a murine model of acute liver failure. Apoptosis **13:**1427–1438.

28. **Lake-Bakaar, G., D. Sorbi, and V. Mazzoccoli.** 2001. Nitric oxide and chronic HCV and HIV infections. Dig. Dis. Sci. **46:**1072–1076.
29. **Li, Y., et al.** 2007. Morphine inhibits intrahepatic interferon-alpha expression and enhances complete hepatitis C virus replication. J. Infect. Dis. **196:**719–730.
30. **Li, Y., et al.** 2003. Morphine enhances hepatitis C virus HCV replicon expression. Am. J. Pathol. **163:**1167–1175.
31. **Lin, W., et al.** 2010. Hepatitis C virus regulates transforming growth factor β1 production through the generation of reactive oxygen species in a nuclear factor kappa B-dependent manner. Gastroenterology **138:**2509–2518.
32. **Lin, W., et al.** 2008. HIV increases HCV replication in a TGF-β1-dependent manner. Gastroenterology **134:**803–811.
33. **Lin, W., et al.** 2011. HIV and HCV cooperatively promote hepatic fibrogenesis via induction of reactive oxygen species and NFκB. J. Biol. Chem. **286:**2665–2674.
34. **Liu, Y., et al.** 2004. CD4-independent infection of astrocytes by human immunodeficiency virus type 1: requirement for the human mannose receptor. J. Virol. **78:**4120–4133.
35. **López-Herrera, A., Y. Liu, M. T. Rugeles, and J. J. He.** 2005. HIV-1 interaction with human mannose receptor (hMR) induces production of matrix metalloproteinase 2 (MMP-2) through hMR-mediated intracellular signaling in astrocytes. Biochim. Biophys. Acta **1741:**55–64.
36. **Mahajan, S. D., et al.** 2005. Morphine exacerbates HIV-1 viral protein gp120 induced modulation of chemokine gene expression in U373 astrocytoma cells. Curr. HIV Res. **3:**277–288.
37. **McCarthy, L. E., and T. J. Rogers.** 2001. Alteration of early T cell development by opioid and superantigen stimulation. Adv. Exp. Med. Biol. **493:**163–167.
38. **Ming-Ju, H., H. Yih-Shou, C. Tzy-Yen, and C. Hui-Ling.** 2011. Hepatitis C virus E2 protein induce reactive oxygen species. ROS-related fibrogenesis in the HSC-T6 hepatic stellate cell line. J. Cell. Biochem. **112:**233–243.
39. **Miyagi, T., et al.** 2000. Morphine induces gene expression of CCR5 in human CEMx174 lymphocytes. J. Biol. Chem. **275:**31305–31310.
40. **Munshi, N., A. Balasubramanian, M. Koziel, R. K. Ganju, and J. E. Groopman.** 2003. Hepatitis C and human immunodeficiency virus envelope proteins cooperatively induce hepatocytic apoptosis via an innocent bystander mechanism. J. Infect. Dis. **188:**1192–1204.
41. **Murakami, T., and N. Yamamoto.** 2010. Role of CXCR4 in HIV infection and its potential as a therapeutic target. Future Microbiol. **5:**1025–1039.
42. **Novick, D. M., et al.** 1985. Hepatic cirrhosis in young adults: association with adolescent onset of alcohol and parenteral heroin abuse. Gut **26:**8–13.
43. **Payabvash, S., et al.** 2006. Chronic morphine treatment induces oxidant and apoptotic damage in the mice liver. Life Sci. **79:**972–980.
44. **Perry, C. M.** 2010. Maraviroc: a review of its use in the management of CCR5-tropic HIV-1 infection. Drugs **70:**1189–1213.
45. **Peterson, P. K., T. W. Molitor, and C. C. Chao.** 1998. The opioid-cytokine connection. J. Neuroimmunol. **83:**63–69.
46. **Raaben, M., G. C. Grinwis, P. J. Rottier, and C. A. de Haan.** 2010. The proteasome inhibitor Velcade enhances rather than reduces disease in mouse hepatitis coronavirus-infected mice. J. Virol. **84:**7880–7885.
47. **Raaben, M., et al.** 2010. The ubiquitin-proteasome system plays an important role during various stages of the coronavirus infection cycle. J. Virol. **84:**7869–7879.
48. **Sacerdote, P.** 2006. Opioids and the immune system. Palliat. Med. **20:**s9–s15.
49. **Satheshkumar, P. S., L. C. Anton, P. Sanz, and B. Moss.** 2009. Inhibition of the ubiquitin-proteasome system prevents vaccinia virus DNA replication and expression of intermediate and late genes. J. Virol. **83:**2469–2479.
50. **Sawa, T., T. Akaike, and H. Maeda.** 2000. Tyrosine nitration by peroxynitrite formed from nitric oxide and superoxide generated by xanthine oxidase. J. Biol. Chem. **275:**32467–32474.
51. **Schaeffer, E., R. Geleziunas, and W. C. Greene.** 2001. Human immunodeficiency virus type 1 Nef functions at the level of virus entry by enhancing cytoplasmic delivery of virions. J. Virol. **75:**2993–3000.
52. **Shields, P. L., et al.** 1999. Chemokine and chemokines receptor interactions provide a mechanism for selective T cell recruitment to specific liver compartments within hepatitis C-infected liver. J. Immunol. **163:**6236–6243.
53. **Soriano, V., E. Vispo, P. Labarga, J. Medrano, and P. Barreiro.** 2010. Viral hepatitis and HIV co-infection. Antiviral Res. **85:**303–315.
54. **Steele, A. D., E. E. Henderson, and T. J. Rogers.** 2003. Mu-opioid modulation of HIV-1 coreceptor expression and HIV-1 replication. Virology **309:**99–107.
55. **Stefano, G. B., M. K. Leung, T. V. Bilfinger, and B. Scharrer.** 1995. Effect of prolonged exposure to morphine on responsiveness of human and invertebrate immunocytes to stimulatory molecules. J. Neuroimmunol. **63:**175–181.
56. **Sulkowski, S. M., and D. L. Thomas.** 2003. Hepatitis C in the HIV-infected person. Ann. Intern. Med. **138:**197–207.
57. **Suzuki, S., L. F. Chuang, P. Yau, R. H. Doi, and R. Y. Chuang.** 2002. Interactions of opioid and chemokine receptors: oligomerization of mu, kappa, and delta with CCR5 on immune cells. Exp. Cell Res. **280:**192–200.
58. **Tardif, K. D., G. Waris, and A. Siddiqui.** 2005. Hepatitis C virus, ER stress, and oxidative stress. Trends Microbiol. **13:**159–163.
59. **Tennant, F., and D. Moll.** 1995. Seroprevalence of hepatitis A, B, C, and D markers and liver function abnormalities in intravenous heroin addicts. J. Addict. Dis. **14:**35–49.
60. **Thomas, D. L.** 2008. The challenge of hepatitis C in the HIV-infected person. Annu. Rev. Med. **59:**473–485.
61. **Thomas, D. L., et al.** 2000. The natural history of hepatitis C virus infection: host, viral, and environmental factors. JAMA **284:**450–456.
62. **Tilton, J. C., and R. W. Doms.** 2010. Entry inhibitors in the treatment of HIV-1 infection. Antiviral Res. **85:**91–100.
63. **Vezali, E., A. Aghemo, and M. Colombo.** 2010. A review of the treatment of chronic hepatitis C virus infection in cirrhosis. Clin. Ther. **32:**2117–2138.
64. **Vlahakis, S. R.** 2006. Human immunodeficiency virus and hepatitis C virus co-infection. J. Med. Liban. **54:**106–110.
65. **Wakita, T., et al.** 2005. Production of infectious hepatitis C virus in tissue culture from a cloned viral genome. Nat. Med. **11:**791–796.
66. **Wang, C. Q., et al.** 2005. Morphine withdrawal enhances hepatitis C virus replicon expression. Am. J. Pathol. **167:**1333–1340.
67. **Wang, J., R. A. Barke, J. Ma, R. Charboneau, and S. Roy.** 2008. Opiate abuse, innate immunity, and bacterial infectious diseases. Arch. Immunol. Ther. Exp. (Warsz.) **56:**299–309.
68. **Wang, X., T. Zhang, and W. Z. Ho.** 2011. Opioids and HIV/HCV Infection. J. Neuroimmune Pharmacol. [Epub ahead of print.] doi:10.1007/s11481-011-9296-1.
69. **Williams, J. P., et al.** 2007. Human peripheral blood mononuclear cells express nociceptin/orphanin FQ, but not mu, delta, or kappa opioid receptors. Anesth. Analg. **105:**998–1005.
70. **Xiao, P., et al.** 2008. Characterization of a CD4-independent clinical HIV-1 that can efficiently infect human hepatocytes through chemokine (C-X-C motif) receptor 4. AIDS **22:**1749–1757.
71. **Zhang, T., et al.** 2003. Interleukin-1β induces macrophage inflammatory protein-1β expression in human hepatocytes. Cell. Immunol. **226:**45–53.
72. **Zhang, T. Y., Q. S. Zheng, J. Pan, and R. L. Zheng.** 2004. Oxidative damage of biomolecules in mouse liver induced by morphine and protected by antioxidants. Basic Clin. Pharmacol. Toxicol. **95:**53–58.
73. **Zhao, L., H. Toriumi, Y. Kuang, H. Chen, and Z. F. Fu.** 2009. The roles of chemokines in rabies virus infection: overexpression may not always be beneficial. J. Virol. **83:**11808–11818.
74. **Zheng, S. J., P. Wang, G. Tsabary, and Y. N. Chen.** 2004. Critical roles of TRAIL in hepatic cell death and hepatic inflammation. J. Clin. Invest. **113:**58–64.
75. **Zhong, J., et al.** 2005. Robust hepatitis C virus infection in vitro. Proc. Natl. Acad. Sci. U. S. A. **102:**9294–9299.